amounts of complex formation (9). These heats of dissociation indicate that heat is absorbed for the dissociation process, while the heat of dilution results indicate that heat is still given off for the total dilution process. The dissociation of rare earth nitrate complexes thus reduces the heats of dilution from the amounts that would occur if no complexed species were present. The shift in the minimum for $\bar{L}_2$ from Pr–Nd (for the perchlorates) to Sm (for the nitrates) and the increase in $\bar{L}_2$ from La to Lu above 2 m in the nitrates are in agreement with what one would expect from stability constant and heat of dissociation data. In addition, the minimum in $\bar{L}_2$ at Sm vanishes by 2 m. This is in agreement with the disappearence of the maximum in the amount of complex formation as deduced from electrical conductance data (12).

A number of other anions form complexes with properties similar to the rare earth nitrates. The rare earth sulfate, EDTA, and thiodiacetate complexes (3, 5, 10, 15) exhibit extrema for the stability constants and/or heats of dissociation of these complexes across the rare earth series. These complexes of the rare earth ions might be expected to show similar series trends in the heats of dilution at low concentrations.

Acknowledgment

Literature Cited

(1) Abrahamer, I., Marcus, Y., *Inorg. Chem.*, **6**, 2103 (1967).
(2) Choppin, G. R., Strazik, W. F., *Inorg. Chem.*, **4**, 1250 (1965).
(3) Dellien, I., Grenthe, I., Hessler, G., *Acta Chem. Scand.*, **27**, 2431 (1973).
(4) Derer, J. L., Ph.D. dissertation, Iowa State University, Ames, Iowa, 1974.
(5) Farrow, M. M., Purdie, N., *J. Solution Chem.*, **2**, 503 (1973).
(6) Garnsey, R., Ebdon, D. W., *J. Am. Chem. Soc.*, **91**, 50 (1969).
(7) Gucker, F. T., Pickard, H. B., Planck, R. W., *J. Am. Chem. Soc.*, **61**, 459 (1939).
(8) Mohs, M. A., Ph.D. dissertation, Iowa State University, Ames, Iowa, 1970.
(9) Moulin, N., Hussonnois, M., Brillard, L., Guillaumont, R., *J. Inorg. Nucl. Chem.*, **37**, 2521 (1975).
(10) Ots, H., *Acta Chem. Scand.*, **27**, 2344 (1973).
(11) Peppard, D. F., Mason, G. W., Hucher, I., *J. Inorg. Nucl. Chem.*, **24**, 881 (1962).
(12) Rard, J. A., Spedding, F. H., *J. Phys. Chem.*, **79**, 257 (1975).
(13) Rard, J. A., Spedding, F. H., Shiers, L. E., Heiser, D. J., unpublished data.
(14) Rossini, F. D., Wagman, D. D., Evans, W. H., Levine, S., Jaffe, I., *Natl. Bur. Stand. (U.S.), Circ.*, No. 500 (1952).
(15) Spedding, F. H., Jaffe, S., *J. Am. Chem. Soc.*, **76**, 882 (1954).
(16) Spedding, F. H., Mohs, M. M., Derer, J. L., Habenschuss, A., *J. Chem. Eng. Data*, in press.
(17) Spedding, F. H., Pikal, M. J., Ayers, B. O., *J. Phys. Chem.*, **70**, 2440 (1966).
(18) Spedding, F. H., Shiers, L. E., Brown, M. A., Baker, J. L., Gutierrez, L., McDowell, L. S., Habenschuss, A., *J. Phys. Chem.*, **79**, 1087 (1975).
(19) Templeton, D. H., Dauben, C. H., *J. Am. Chem. Soc.*, **76**, 5237 (1954).

Solubilities of Heavy Hydrocarbons in Compressed Methane and Nitrogen

Saul G. D'Avila,[†] Bal K. Kaul, and John M. Prausnitz*

Chemical Engineering Department, University of California, Berkeley, California 94720

Vapor-phase solubilities of n-decane, 2,2,5-trimethylhexane, tert-butylbenzene, and n-dodecane were measured in compressed methane and in compressed nitrogen. Measurements were taken in the range 30–100 atm and 25–125 °C. From these measurements, second virial cross coefficients B_{12} were calculated with a maximum uncertainty of ± 10 cm^3 mol^{-1}.

Interactions between molecules of common nonpolar gases (e.g., N_2 and methane) are now reasonably well understood but little is known about the interactions of such gases with large hydrocarbons. An understanding of these interactions is becoming of increasing importance in technology as development of new processes concerned with gasification of coal and heavy petroleum is stimulated by changes in the world's energy supply.

In several recent publications from this laboratory, experimental solubility data were reported for a number of gaseous solutes in heavy hydrocarbon solvents (3, 4, 11). These data, in the form of Henry's constants, supply fundamental information

† Now at Departamento de Engenharia Quimica, Universidade de Campinas, 13100 Campinas, Brazil.

on the behavior of a small molecule (e.g., methane) when it is completely surrounded by large hydrocarbon molecules in the liquid phase. In the work presented here, we report some experimental solubility data on the other end of the composition spectrum: the behavior of a large hydrocarbon molecule completely surrounded by small molecules in the gas phase. These data, in the form of second virial cross coefficients, give fundamental information on the potential energy function for dissimilar molecules. More important for technological application, these data are useful for estimating solvent losses in high-pressure absorbers and for estimating dew points in gas mixtures containing small amounts of heavy hydrocarbon components such as tars.

Experimental Section

The experimental technique used for solubility measurements is essentially the same as that used by Rigby (10) and Benson (2). Figure 1 presents a schematic diagram of the apparatus. Hydrocarbon liquid is placed in each of two equilibrium cells, arranged in series. High-pressure gas, entering through spargers at the bottom of each cell, slowly bubbles through the liquid; the gas leaving the second equilibrium cell is saturated with the heavy component. Two cells in series are used to assure saturation. The high-pressure, gas-phase mixture leaving the second
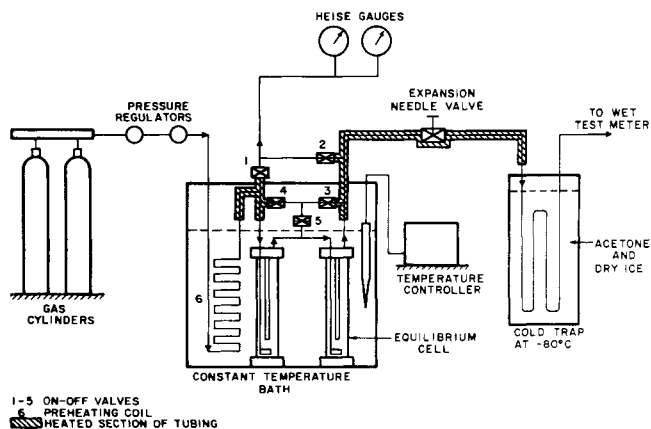
Figure 1. Schematic diagram of solubility apparatus.

Table I. Solubilities of Liquids in Compressed Nitrogen

Liquid component 2	Temp, °C	Total pressure, atm	Vapor-phase mole fraction $10^4 y_2$
n-Decane	50	41.7	4.16
	50	51.0	3.95
	50	91.0	4.27
	75	31.5	15.00
	75	38.0	14.10
	100	87.4	27.00
	100	100.6	27.10
	125	70.4	65.70
	125	99.6	61.60
2,2,5-Trimethylhexane	25	67.2	8.85
	25	75.5	8.40
	25	83.4	9.62
	50	69.7	25.30
	50	79.4	26.20
	75	65.3	63.60
	75	75.0	62.10
	100	70.4	139.0
	100	84.5	128.0
tert-Butylbenzene	50	66.3	4.84
	50	82.5	4.92
	50	100.4	4.94
	75	72.3	13.80
	75	90.4	14.00
	100	72.5	34.7
	100	82.8	33.4
	125	74.4	74.8
	125	82.6	69.8
n-Dodecane	75	71.2	2.33
	75	78.3	2.39
	75	83.7	2.19
	100	78.5	6.70
	100	90.1	7.02
	125	78.5	16.2
	125	90.2	17.2
	150	70.1	39.0
	150	92.7	41.7

Table II. Solubilities of Liquids in Compressed Methane

Liquid component 2	Temp, °C	Total pressure, atm	Vapor-phas mole fraction $10^4 y_2$
n-Decane	50	60.1	5.58
	50	74.1	6.28
	50	105.2	9.53
	75	88.2	17.1
	75	107.8	21.9
	100	72.5	35.7
	100	88.2	37.8
	125	75.4	70.1
	125	84.8	71.8
2,2,5-Trimethylhexane	25	75.2	12.6
	25	81.2	13.3
	25	90.1	15.1
	50	68.6	35.3
	50	80.9	33.1
	75	79.5	81.8
	75	90.2	77.2
	100	72.5	163.0
	100	87.3	166.0
tert-Butylbenzene	50	73.2	7.32
	50	84.5	8.36
	50	100.4	10.5
	75	73.4	19.9
	75	86.8	19.3
	100	88.1	46.2
	100	101.3	49.2
	125	85.2	86.4
	125	100.2	84.3
n-Dodecane	75	76.8	4.13
	75	85.3	4.16
	75	92.1	4.51
	100	76.5	11.6
	100	85.3	11.7
	125	77.5	25.1
	125	90.1	23.7
	150	77.3	54.7
	150	90.2	51.0

equilibrium cell is then expanded; the condensable component is removed by a cold trap, a mixture of acetone and dry ice at −80 °C. The volumetric flow rate, measured with a wet-test meter, was typically 50 cm³ min⁻¹. The accuracy of the flow measurement is within 0.1%. The condensate, determined gravimetrically, ranged from 1 to 4 g.

Downstream from the equilibrium cells, glass wool was used to eliminate entrainment. Experimental studies verified that the measured solubilities are independent of flow rate.

The equilibrium cells were placed in a constant-temperature bath controlled to ±0.05 °C. The temperature of the liquid in the cells was measured to ±0.1 °C with a copper–constantan thermocouple calibrated with a National Bureau of Standards thermometer. The bath fluid was dimethylpolysiloxane (Dow Corning 200 Fluid).

Pressure in the second equilibrium cell was measured to ±0.5 psia with a Bourdon-tube Heise pressure gauge calibrated with an Aminco dead-weight gauge.

Methane gas (99% purity) was obtained from Matheson Inc. and high-purity nitrogen gas was obtained from Liquid Carbonic Corporation. n-Decane and n-dodecane were obtained from Phillips Petroleum Company; tert-butylbenzene from Matheson, Coleman and Bell Co., and 2,2,5-trimethylhexane was supplied by Chemical Sample Company. All liquids had a reported purity of at least 99% as checked by gas–liquid-chromatography measurements. For all gases, water content was less than 10 ppm.

Results

Table I presents solubilities of n-decane, 2,2,5-trimethylhexane, tert-butylbenzene, and n-dodecane in compressed nitrogen. Table II presents those in compressed methane.

Data Reduction

To calculate the second virial cross coefficient from solubility data we find the vapor-phase fugacity coefficient ϕ.

Consider the equilibrium relation for liquid (component 2) at temperature T, and total pressure P:

$$f_2^V = f_2^L \tag{1}$$

Table III. Second Virial Cross Coefficients B_{12} for Eight Binary Systems

Components	Temp, °C	$-B_{12}$, cm^3 mol^{-1}
Nitrogen–n-decane	50	148
	75	111
	100	82
	125	74
Methane–n-decane	50	289
	75	232
	100	181
	125	134
Nitrogen–2,2,5-trimethylhexane	25	115
	50	93
	75	73
	100	52
Methane–2,2,5-trimethylhexane	25	243
	50	200
	75	169
	100	144
Nitrogen–$tert$-butylbenzene	50	111
	75	83
	100	70
	125	49
Methane–$tert$-butylbenzene	50	224
	75	179
	100	158
	125	120
Nitrogen–n-dodecane	75	134
	100	104
	125	74
	150	53
Methane–n-dodecane	75	290
	100	248
	125	200
	150	164

where superscript V stands for vapor phase and superscript L for liquid phase. The fugacities f are related to mole fractions y and x by

$$f_2^V = \phi_2 y_2 P \tag{2}$$

$$f_2^L = \gamma_2^L (1 - x_l) P_2^s \phi_2^s \exp\left[\frac{v_2^L (P - P_2^s)}{RT}\right] \tag{3}$$

where v^L is the molar liquid volume and subscript l refers to the light component. Superscript s refers to the pure saturated fluid at system temperature T.

Substitution gives for the fugacity coefficient

$$\phi_2 = \frac{\gamma_2^L (1 - x_l) P_2^s \phi_2^s \exp\left[\dfrac{v_2^L (P - P_2^s)}{RT}\right]}{y_2 P} \tag{4}$$

Solubility x_l was calculated (or estimated) from direct solubility data (3, 4, 11). Since $x_l \ll 1$, it is not necessary that x_l be known accurately. Further, since $x_l \ll 1$, γ_2^L is near unity. To estimate γ_2^L we used regular solution theory coupled with a Flory-Huggins entropy correction (9).

The vapor pressure of the liquid in the working temperature range is small; therefore the fugacity coefficient ϕ_2^s of the pure liquid at saturation pressure is essentially unity. Vapor pressures and molar liquid volumes were taken from the literature (1).

The fugacity coefficient in the vapor phase is given by the virial equation (9):

$$\ln \phi_2 = \frac{2}{v} (y_2 B_{22} + y_1 B_{12}) - \ln z \tag{5}$$

where v is the molar volume and z is the compressibility factor of the saturated gas:

$$z = \frac{Pv}{RT} = 1 + \frac{1}{v} [y_1^2 B_{11} + 2y_1 y_2 B_{12} + y_2^2 B_{22}] \tag{6}$$

Since $y_2 \ll y_1$, eq 5 shows that the fugacity coefficient is very sensitive to B_{12}. Reliable measurements of y_2, therefore, yield accurate values of B_{12}. Further, z and v are essentially those for the pure gas (methane or nitrogen) for which very good experimental data are a vailable (5, 6). However, corrections in v and z were made as indicated by eq 6. Since $y_2 \ll y_1$, an approximate value for B_{22} is sufficient. The desired coefficient B_{12} is found by iteration but convergence is extremely fast.

Table III presents second virial cross coefficients calculated from solubility data. Considering experimental uncertainties, the effect of higher terms in the virial expansion, as well as possible errors in estimation of $(1 - x_l)$ and γ_2^L, we believe that the results shown in Table III have a precision of about ± 10 cm^3 mol^{-1}.

The results shown in Table III are significantly smaller in magnitude than those predicted by the correlations of Pitzer and Curl (8) and McGlashan and Wormald (7) using conventional mixing rules. The experimental results are typically more positive than those predicted by 50–100 cm^3 mol^{-1}. This discrepancy is not surprising since the correlations were not developed for second virial cross coefficients but for pure fluids and for these, the data used to establish the correlations refer to smaller hydrocarbons, with carbon numbers primarily below 7. The theorem of corresponding states, even as amended by Pitzer's introduction of the acentric factor, was never intended to be applicable for large molecules; the acentric factor gives only a first-order perturbation to the two-parameter corresponding states theory for simple, spherical (argon-like) molecules.

Experimental data, similar to those given here, are now being obtained for binary mixtures containing, as the heavy component, hydrocarbons of still higher carbon number. When accumulation of these data is completed, we shall have established an empirical base for attempting a theoretical correlation of second virial cross coefficients for binary mixtures containing small and large molecules.

Glossary

B	second virial coefficient, cm^3 mol^{-1}
f	fugacity
P	total pressure
P^s	vapor pressure
R	gas constant
T	absolute temperature
v	molar volume
x	mole fraction in liquid phase
y	mole fraction in gas phase
γ	activity coefficient in liquid phase
ϕ	fugacity coefficient in gas phase

Subscripts

1, 2	components

Superscripts

L	liquid phase
V	gas phase
s	pure component at saturation

Literature Cited

(1) API Project 44, Selected Values of Properties of Hydrocarbons and Related Compounds, Vol. II. and Vol. IV, Thermodynamic Research Center, Texas, 1975.
(2) Benson, P. R., Prausnitz, J. M., AIChE J., **5**, 161 (1959).
(3) Chappelow, C. C., Prausnitz, J. M., AIChE J., **20**, 1097 (1974).
(4) Cukor, P. M., Prausnitz, J. M., J. Phys. Chem. **76**, 598 (1971).

(5) Goodwin, R. D., Natl. Bur. Stand. (U.S.), Tech. Note, 653 (1974).
(6) Jacobsen, R. T., Stewart, R. B., Natl. Bur. Stand. (U.S.), Tech. Note, 648 (1973).
(7) McGlashan, M. L., Wormald, C. J., Trans. Faraday Soc., 60, 646 (1964).
(8) Pitzer, K. S., Curl, R. F., J. Am. Chem. Soc., 79, 2369 (1957).
(9) Prausnitz, J. M., "Molecular Thermodynamics of Fluid-Phase Equilibrium", Prentice-Hall, Englewood Cliffs, N.J., 1968, Chapter 5.

(10) Rigby, M., Prausnitz, J. M., J. Phys. Chem., 72, 330 (1968).
(11) Tremper, K. K., Prausnitz, J. M., J. Chem. Eng. Data, 21, 295 (1976).

Activity Coefficients at Infinite Dilution: Alcohols and Esters in n-Hexadecane, Alcohols in Ethyl Octanoate, and Esters in 1-Octadecanol

V. John Comanita, Robert A. Greenkorn, and Kwang-Chu Chao*

School of Chemical Engineering, Purdue University, West Lafayette, Indiana 47907

Gas–liquid partition chromatography was used to determine infinite dilution activity coefficients in binary liquid solutions at 100–140 °C. The binary systems studied are: alcohols and esters in n-hexadecane, alcohols in ethyl octanoate, and esters in 1-octadecanol.

Infinite dilution activity coefficients in binary solutions are important quantities in solution thermodynamics. They define useful boundary conditions in the integration of the Gibbs–Duhem equation, and are therefore valuable for the description of the solution behavior of the entire binary solution system. Schreiber and Eckert (5) showed that the Wilson equation gives consistently reliable results when the equation constants are determined from infinite dilution activity coefficients and the same results hold when the equation is extended to multicomponent systems.

In this work we determine the infinite dilution activity coefficients in a number of systems: methanol, ethanol, propanol, and 1-butanol in n-hexadecane and in ethyl octanoate; methyl acetate, methyl propionate, and ethyl propionate in n-hexadecane and in 1-octadecanol. The molecules studied contain structural groups of wide interest. We are interested in determining the interaction properties of these groups from analysis of these and other data. Meanwhile the present data can be of direct interest for the description of the behavior of the binary solutions studied.

The gas–liquid partition chromatograph and experimental procedure that we used in this work have been described (1, 6). Retention time was determined as the elapsed time required by the injected solute to travel through the chromatograph column in which the packing was loaded with the solvent. The solute was carried by the helium elution gas through a conductivity cell both before and after passing through the chromatograph column. The time of the conductivity cell output peak was recorded as a digital signal accurate to 0.1 s. The equilibrium vaporization ratio K of the solute was obtained from the retention time and was found to be reproducible to about 3%.

The column temperature is controlled to within ± 0.25 °C, pressure to ± 0.02 atm, and flow rate to 2%. Detailed error analysis of the contributing factors showed the uncertainty of the measured K values to be about 3% in agreement with the directly observed uncertainty.

K values were obtained from the direct experimental observables by

$$K_i = \frac{nz_a}{p_a F_a (t_{R_i} - t_g)} \, RT_a \tag{1}$$

The equation has been described (6). The symbols are explained in the glossary section. K values were determined at four pressures for each temperature. Figure 1 illustrates the results with propanol in n-hexadecane.

From plots like Figure 1 interpolation was made to obtain K values at a conveniently low pressure, fixed at 1.7 atm in this
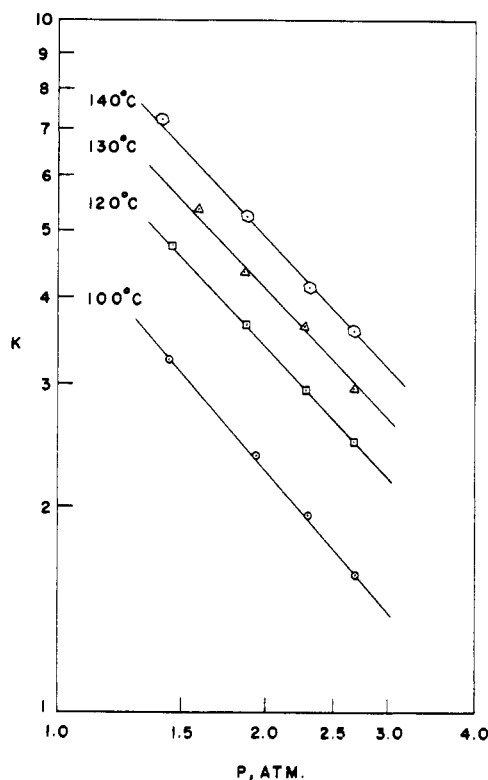

Figure 1. K values of propanol at infinite dilution in He–n-hexadecane.